Carbon Nanodots, Ru Nanodots and Hybrid Nanodots: Preparation and Catalytic Property

Article *in* Journal of Materials Chemistry A · June 2015

DOI: 10.1039/C5TA03355A

3 authors:

Abhijit Biswas
Indian Association for the Cultivation of Science
8 PUBLICATIONS **542** CITATIONS
SEE PROFILE

Subir Paul
Indian Association for the Cultivation of Science
13 PUBLICATIONS **213** CITATIONS
SEE PROFILE

Arindam Banerjee
Indian Association for the Cultivation of Science
166 PUBLICATIONS **7,045** CITATIONS
SEE PROFILE

Journal of Materials Chemistry A

PAPER

View Article Online
View Journal | View Issue

Cite this: J. Mater. Chem. A, 2015, 3, 15074

Carbon nanodots, Ru nanodots and hybrid nanodots: preparation and catalytic properties†

Abhijit Biswas, Subir Paul and Arindam Banerjee*

Received 7th May 2015
Accepted 8th June 2015

DOI: 10.1039/c5ta03355a

www.rsc.org/MaterialsA

New hybrid nanodots comprised of carbon nanodots and ruthenium nanodots have been synthesized from peptide functionalized carbon nanodots and a ruthenium salt. At first, carbon nanodots have been prepared by carbonization of a synthetic tripeptide and citric acid. Then these functionalized carbon nanodots act as a template to form ruthenium nanodots from a ruthenium salt in the presence of a reducing agent, sodium borohydride in water medium. These functionalized carbon nanodots exhibit a blue emission with a high quantum yield (69.8%). Various techniques including UV-Vis, fluorescence, FTIR, X-ray photoelectron spectroscopy (XPS), Raman and X-ray diffraction and transmission electron microscopy (TEM) analyses have been used to characterize carbon nanodots and hybrid nanodots. This is a new example of preparing ruthenium nanodots by using peptide functionalized carbon nanodots as a stabilizer to form unique hybrid nanodots consisting of carbon nanodots and ruthenium nanodots in water medium. Moreover, hybrid nanodots act as a potential catalyst for the reduction of organic azides to their corresponding amines in aqueous medium. A variety of functionalized organic azides have been reduced to their corresponding amines with high yields without affecting other functionalities indicating the good chemoselectivity of the catalyst towards the azide functionality.

Introduction

Over the past several years, carbon based nanomaterials including carbon nanodots, fullerene, nanodiamonds, carbon nanotubes and graphene have been considered as an active area of research.[1–14] Among these nanomaterials, carbon nanodots have emerged as a very promising and a new class of carbogenic nanomaterials due to their fascinating intrinsic properties.[15–18] This has prompted to develop a series of synthetic procedures for carbon nanodots from low cost carbon containing materials over the years.[19–26] Carbon nanodots are endowed with many interesting properties including high aqueous dispersibility, robust chemical inertness, on demand functionalization, high resistance to photo-bleaching, low toxicity, good biocompatibility and multi-color emissive properties. These make them wonderful candidates for applications in bioimaging, catalysis, multi-color printing, sensing, and others.[27–38] In spite of these aforementioned applications, carbon nanodots have been rarely used as a template for the synthesis of other nanoparticles/nanodots to obtain a hybrid nanomaterial.[39] Hybrid nanomaterials belong to an interesting class of nanomaterials owing to their fascinating properties that are different from their individual constituent(s).[40] Though there are some examples of hybrid nanomaterials,[41–43] construction of hybrid nanodots with carbon nanodots as a constituent still remains a great challenge. So, there is a real need to explore the possibility of newly synthesized carbon nanodots as a template for preparing other nanoparticles/nanodots. In this study, we have prepared surface functionalized highly fluorescent (blue emitting) carbon nanodots through the one step hydrothermal treatment of a unique precursor and this precursor is prepared from treatment of citric acid and a tripeptide, Gly-Gly-DNDn (GGDn), (DNDn = 12-aminododecanoic acid). Scheme 1 illustrates the synthesis of carbon nanodots from their precursor. Transition metal elements draw special attention in their respective nano-form owing to the exceptional enhancement of their catalytic properties at the nanoscale.[44] Among these transition metal elements, there are only a few methods in the literature for preparing ruthenium nanoparticles.[45–50] However, there is no report regarding the synthesis of ruthenium nanodots by using carbon nanodots to the best of our knowledge. This study demonstrates the first report of using peptide functionalized carbon nanodots as a template for the synthesis of ruthenium nanodots from a ruthenium salt in the presence of a reducing agent, sodium borohydride. In this study, peptide functionalized carbon nanodots not only assist in the formation of ruthenium nanodots but also stabilization of these ruthenium nanodots. This is a convincing demonstration of preparing organic (peptide functionalized carbon nanodots)–inorganic (ruthenium nanodots) hybrid nanodots by using a novel strategy. Furthermore, these Ru based hybrid nanodots have

Department of Biological Chemistry, Indian Association for the Cultivation of Science, Jadavpur, Kolkata-700032, India. E-mail: bcab@iacs.res.in; Fax: +91-33-2473-2805

† Electronic supplementary information (ESI) available. See DOI: 10.1039/c5ta03355a

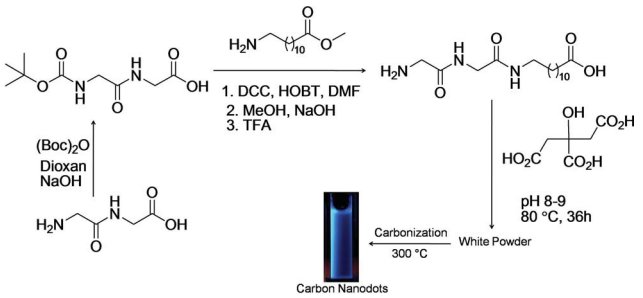

Scheme 1 Schematic representation of the formation of carbon nanodots by carbonization of Gly-Gly-DNDn.

been explored as a potential catalyst in water medium for the transformation of organic azides to their corresponding amines and these amines are extensively used in pharmaceutical, chemical and biological sciences.[51–53] Among the several synthetic routes to prepare organic amines, the azide reduction is the most efficient protocol. This is due to the fact that organic azides are easily accessible and it is a straightforward route to reduce an azide to its corresponding amine. Though there are a few examples of using metal, metal oxide and semiconducting nanoparticles as catalysts for azide to amine transformation,[54–56] Ru(0) nanodots have not yet been explored as a catalyst for the azide to amine reduction. In our strategy, the hybrid nanodots containing carbon nanodots and Ru nanodots have been successfully utilised as an efficient catalyst to reduce various organic azides (containing other functional groups) to their corresponding amines without affecting other functional groups in the presence of hydrazine monohydrate in water medium.

Experimental section

Reagents and materials

Sodium hydroxide, di-*tert*-butyl pyrocarbonate, HOBt·H_2O (1-hydroxybenzotriazole monohydrate), DCC (*N*,*N*′-dicyclohexylcarbodiimide), glycylglycine and solvents were purchased from SRL, India. Other materials were purchased from Sigma-Aldrich.

General methods for synthesis of the peptide

The tripeptide was synthesized by conventional solution phase methods by using a racemization free fragment condensation strategy. The Boc group was used for the N-terminal protection and the C-terminus was protected as a methyl ester. Coupling was mediated by *N*,*N*-dicyclohexylcarbodiimide and 1-hydroxybenzotriazole monohydrate (DCC/HOBt·H_2O). The C-terminal methyl group was deprotected by using aqueous sodium hydroxide. The final compound was fully characterized by mass spectrometry, ^{1}H NMR spectroscopy and ^{13}C NMR spectroscopy.

Synthesis of Boc-Gly-Gly-OH

1.32 g (10 mmol) of glycylglycine was taken in a round bottomed flask. Then 10 mL 1 (N) NaOH, 10 mL water and 20 mL 1, 4-dioxane were added to it and cooled to 0 °C. 2.20 g (10.1 mmol) di-*tert*-butyl dicarbonate (Boc anhydride) was added to the reaction mixture and stirred for 10 hours at room temperature. Then the volume of the solution was reduced to one third in a vacuum. The resulting mixture was acidified with saturated $KHSO_4$ solution and the aqueous layer was extracted with ethyl acetate (3 × 40 mL). The ethyl acetate extract was dried over anhydrous sodium sulfate and evaporated in a vacuum to obtain the white powdered product. Yield: 2.106 g (9.07 mmol, 90.76%).

Synthesis of Boc-Gly-Gly-DNDn-OMe

2.106 g (9.07 mmol) of Boc-Gly-Gly-OH was dissolved in 12 mL dry *N*,*N*-dimethyl formamide (DMF) and cooled in an ice bath. H-DNDn-OMe (DNDn = 12-aminododecanoic acid) was obtained by neutralization with saturated Na_2CO_3 from its hydrochloride salt and subsequent extraction with ethyl acetate. The ethyl acetate solution was then concentrated to 10 mL and added to the DMF solution followed by 1.38 g (9.04 mmol) of HOBt·H_2O and 1.95 g (9.5 mmol) of *N*,*N*-dicyclohexylcarbodiimide (DCC). The reaction mixture was then allowed to reach room temperature and stirred for 24 hours. The reaction mixture was diluted with ethyl acetate and filtered to separate *N*,*N*-dicyclohexylurea (DCU). The ethyl acetate layer was washed with 1(N) HCl (3 × 30 mL), brine (2 × 30 mL), saturated sodium carbonate solution (2 × 30 mL) and brine (2 × 30 mL). The organic layer was dried over anhydrous sodium sulfate and evaporated to obtain the yellowish product. The product was purified through silica gel column chromatography using pet ether/ethyl acetate (5 : 3) as an eluent to obtain the pure white product.

Yield: 2.63 g (5.94 mmol, 65.49%); ^{1}H NMR (500 MHz, $CDCl_3$, δ): 7.016 (br,1H), 6.505 (br, 1H), 5.355 (br, 1H), 3.934–3.922 (d, J = 6Hz, 2H), 3.813–3.802 (d, J = 5.5Hz, 2H), 3.654 (s, 3H), 3.243–3.193 (m, 2H), 2.308–2.270 (m, 2H), 1.618–1.582 (m, 2H), 1.503–1.442 (m, 11H), 1.258–1.243 (m, 14H); ^{13}C NMR (125 MHz, $CDCl_3$, δ): 174.49, 170.16, 168.71, 80.75, 51.56, 44.65, 43.25, 39.89, 34.25, 29.58, 29.55, 29.50, 29.36, 29.34, 29.25, 28.45, 26.99, 25.08; HRMS (*m*/*z*): 466.49 $[M + Na]^+$, 482.48 $[M + K]^+$.

Synthesis of Boc-Gly-Gly-DNDn-OH

2.63 g (5.94 mmol) of Boc-Gly-Gly-DNDn-OMe was taken in a round bottomed flask and dissolved in 50 mL methanol. 15 mL of 1 (N) NaOH was added to it and kept under stirring for 6 hours. The progress of hydrolysis was monitored by thin layer chromatography (TLC). After the completion of the reaction, as indicated by TLC, the methanol was removed in a vacuum. The aqueous part was then taken in 50 mL water and washed with diethyl ether (2 × 30 mL). The remaining solution was acidified with 1 (N) HCl and extracted with ethyl acetate (3 × 40 mL). The ethyl acetate extract was dried over anhydrous sodium sulfate and evaporated in a vacuum to obtain a white powdered product.

Yield: 2.44 g (5.71 mmol, 96.12%); ^{1}H NMR (500 MHz, DMSO-D_6, δ): 12.223 (br, 1H), 7.793–7.766 (m, 1H), 6.472–6.450 (m, 2H), 3.717–3.672 (m, 2H), 3.585–3.571 (m, 2H), 3.036–2.987

(m, 2H), 2.187–2.150 (m, 2H), 1.475–1.442 (m, 2H), 1.357 (s, 11H), 1.059 (s, 14H); ^{13}C NMR (125 MHz, DMSO-D_6, δ): 174.35, 172.29, 169.45, 157.84, 42.79, 41.47, 38.39, 33.65, 29.01, 28.87, 28.82, 28.65, 28.46, 26.30, 24.43; HRMS (m/z): 430.41 $[M + H]^+$, 452.38 $[M + Na]^+$, 468.38 $[M + K]^+$.

Synthesis of H-Gly-Gly-DNDn-OH

At first, 10 mL of trifluoroacetic acid (TFA) was added to 2.44 g (5.71 mmol) of Boc-Gly-Gly-DNDn-OH and removal of the Boc group was monitored by TLC. After 8 h, TFA was removed under vacuum. The residue was taken in water (20 mL) and covered with ethyl acetate (about 50 mL) and basified with a solution of $NaHCO_3$. The aqueous phase was extracted with ethyl acetate and this operation was carried out repeatedly. Ethyl acetate extracts were pooled, washed with water and dried over anhydrous Na_2SO_4 and evaporated in a vacuum. A white material of the peptide H-Gly-Gly-DNDn-OH was obtained as a final product.

Yield: 1.77 g (5.40 mmol, 93.58%); ^{1}H NMR (500 MHz, DMSO-D_6, δ): 12.126 (br, 1H), 7.110–7.092 (m, 1H), 6.468–6.445 (m, 1H), 3.932–3.872 (m, 2H), 3.656–3.525 (m, 2H), 3.073–3.023 (m, 2H), 2.184–2.155 (m, 2H), 1.488–1.461 (m, 2H), 1.369–1.355 (m, 2H), 1.245–1.167 (m, 14H); ^{13}C NMR (125 MHz, DMSO-D_6, δ): 174.87, 168.64, 167.84, 149.36, 139.26, 43.92, 43.89, 41.94, 35.51, 31.41, 31.12, 25.81, 25.62, 25.03; HRMS (m/z): 330.04 $[M + H]^+$, 352.07 $[M + Na]^+$, 368.04 $[M + K]^+$.

Preparation of carbon nanodots

For the synthesis of carbon nanodots, initially 5 equivalents of peptide (GGDn) were taken in water (5 mL) and the pH of the solution was adjusted to 8–9. After that 2 mL of citric acid solution (5 equivalents) was added to this mixture in order to maintain 1 : 1 molar ratio of citric acid: peptide and this mixture was stirred for a few minutes. The sticky mass was collected and dried in a hot oven at 80 °C for 36 hours. The solid was then transferred to a poly (tetrafluoroethylene) (Teflon)-lined autoclave and heated at 300 °C for 2 h. The brownish black product was extracted with 25 mL of hot water and sonicated. The mixture was centrifuged to remove any insoluble particle and the supernatant aqueous solution was collected. The deep brown solution was then precipitated after the addition of acetone at 1 : 10 volume ratio and the supernatant was collected. This supernatant was centrifuged at 14 000 rpm for 1 h to precipitate out the carbon nanodots. The supernatant was removed and the precipitated brownish black mass was further dried in a hot oven at 80 °C until it became powder in nature.

Preparation of carbon nanodot supported ruthenium nanodots and general experimental procedure for the reduction of azides to amines

At first, $RuCl_3 \cdot 3H_2O$ (0.5 equiv) was dispersed in aqueous solution of carbon nanodots (10 mL). Then, sodium borohydride (0.8 equiv) was added to it with vigorous stirring for a few minutes to obtain Ru nanodots. The black solid Ru nanodots were further washed with water and used in azide reduction. The azide compound (1 equiv) and hydrazine monohydrate (5 equiv) were added to the solution mixture containing Ru nanodots as a catalyst in 5 mL of water. The reaction mixture was then refluxed at 100 °C with stirring until the completion of the reaction. The entire procedure was conducted in an inert atmosphere. After the completion of the reaction (checked by TLC) the mixture was extracted with ethyl acetate (3 × 10 mL). The extract was washed thoroughly with water and brine. Then it was dried over Na_2SO_4. The crude product was purified by column chromatography over the silica gel to afford the pure amine product, which was properly characterized by ^{1}H and ^{13}C NMR spectroscopy.

Results and discussion

Carbon nanodots (CNDs) have been synthesized by hydrothermal oxidation of the citric acid–GGDn composite at 300 °C. At first, the citric acid and the peptide GGDn were condensed and then carbonized to prepare fluorescent CNDs. In this study, citric acid acts as a source of the carbon core and the peptide moiety surrounds the surface of CNDs. The attachment of the peptide provides a surface modifier and this is attributed to the water solubility and stability of the CNDs. These CNDs show a bright blue fluorescence upon the excitation at 365 nm using a UV-torch. The calculated fluorescence quantum yield is 69.8% relative to quinine sulfate (as a reference). This indicates that these as-prepared CNDs are strongly fluorescent materials. Experimental studies show that the quantum yield is strongly affected by several factors, the type and number of functional groups present, carbonization time and temperature. It has been found that on changing the substrate from citric acid to malic acid, the % of quantum yield decreases to 6.5%. We have also varied the peptide residue from Gly-Gly-DNDn to Gly-Gly (GG). However, no such considerable change of quantum yield has been observed. The temperature and time are also important factors for tuning the quantum yield. Under optimized conditions, the citric acid–GGDn combination has given the

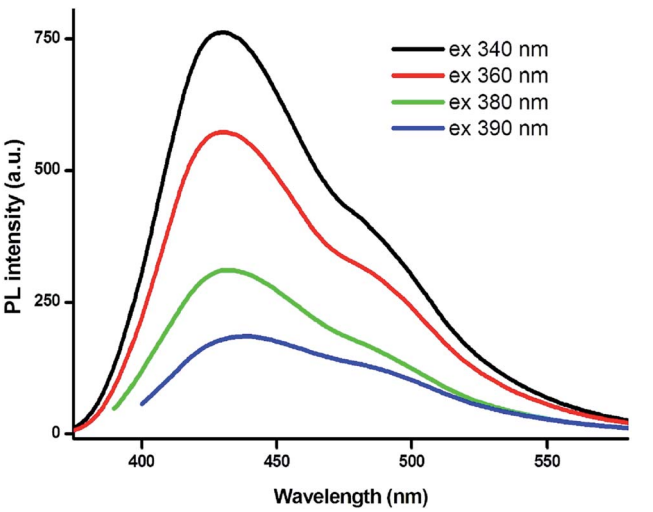

Fig. 1 Fluorescence emission spectra of aqueous solution of carbon nanodots at different excitation wavelengths.

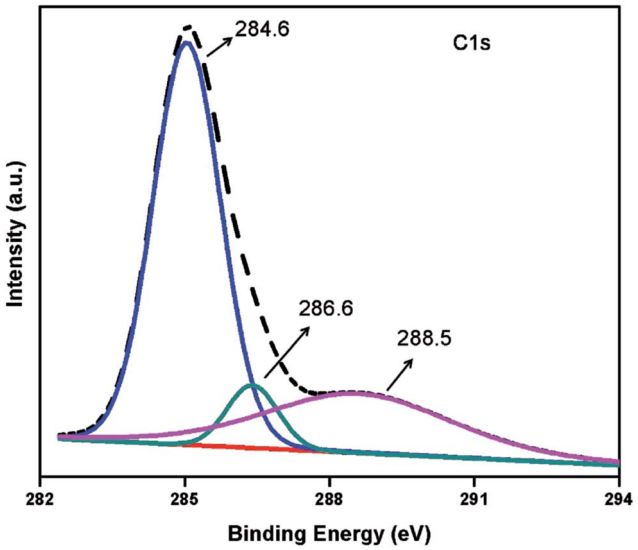

Fig. 2 XPS spectra of carbon nanodots.

maximum quantum yield (69.8%). The entire observation is summarized in Table S1 (ESI†).

Characterization of carbon nanodots

In order to characterize the carbon nanodots, UV-Vis and fluorescence spectroscopy analyses, Transmission Electron Microscopic (TEM), Raman and X-ray Photoelectron Spectroscopic (XPS) spectral analyses have been conducted. It is clearly observed in the UV-Vis study (Fig. S1, ESI†) that the CNDs show a strong absorption at 340 nm. The absorption at 340 nm is due to the $n \rightarrow \pi^*$ transition corresponding to the CNDs. The excitation dependent fluorescence emission spectrum has also been observed (Fig. 1). The fluorescence emission spectra are stable up to an excitation at 380 nm. However, from the excitation at 390 nm, the emission spectrum has started to shift in the longer wavelength with a considerable decrease in intensity. This excitation dependent emission is common in CNDs. In the FTIR spectrum (Fig. S2, ESI†), the characteristic peak at 3380 cm^{-1} is due to the O–H stretching

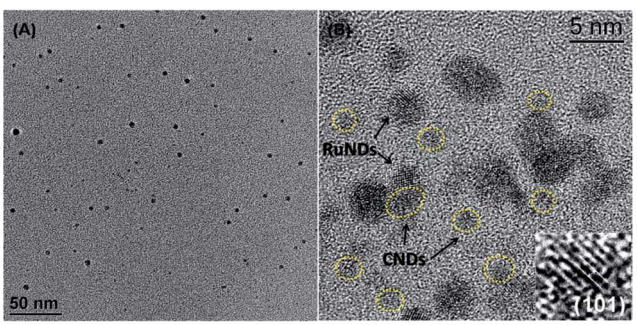

Fig. 3 TEM images of (A) carbon nanodots (CNDs) and (B) ruthenium nanodots (RuNDs) in association with CNDs. The inset in (B) shows the enlarged image of a single ruthenium nanodot indicating lattice fringes.

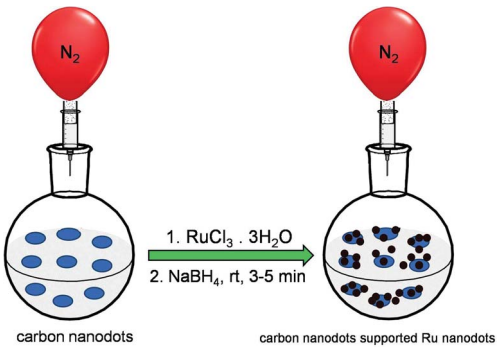

Scheme 2 Schematic representation of the formation of carbon nanodot stabilized Ru nanodots in aqueous medium at room temperature.

mode, while peaks at 1656 cm^{-1} and 1556 cm^{-1} correspond to the amide-I and amide-II peaks of the amide (–NH–CO-) linker present in the CNDs. The peak at 1350 cm^{-1} is assigned to the C–H deformation of CH_2. The peak in the region of 1250-1320 cm^{-1} corresponds to the C–O stretching. These structural analyses (the coexistence of O–H, C=O and C–O functionalities) indicate the presence of the carboxyl moieties on the surface of the CNDs. Moreover, XPS analysis has also been carried out to confirm the surface composition of the CNDs (Fig. 2). The C1s spectra show that peaks at 284.6 eV and 286.6 eV correspond to the binding energy of C–C/C=C and C–O bonds, respectively. The peak at 288.5 eV is attributed to the carboxylic groups. These XPS data are in good agreement with the FTIR analysis. The TEM image (Fig. 3A) reveals that these particles are spherically symmetrical. The average size of CNDs is 2.48 nm. It is also observed that they are amorphous in nature as there is no well resolved lattice plane. The amorphous nature of the CNDs is also supported by Raman spectral analysis (Fig. S3, ESI†). No D or G bands have been obtained in the Raman spectra. In the XRD pattern there is only a broad

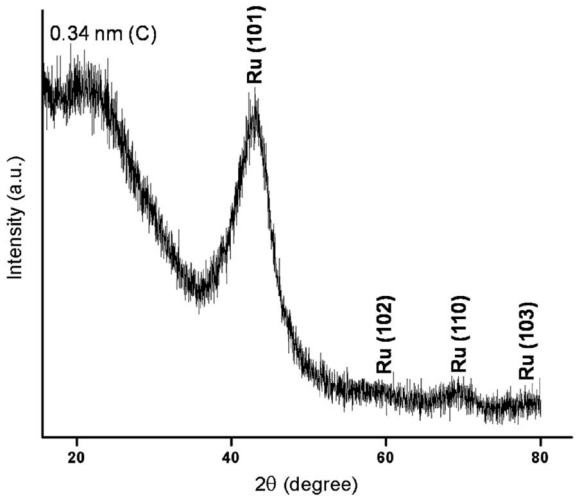

Fig. 4 XRD pattern of ruthenium nanodots supported on carbon nanodots.

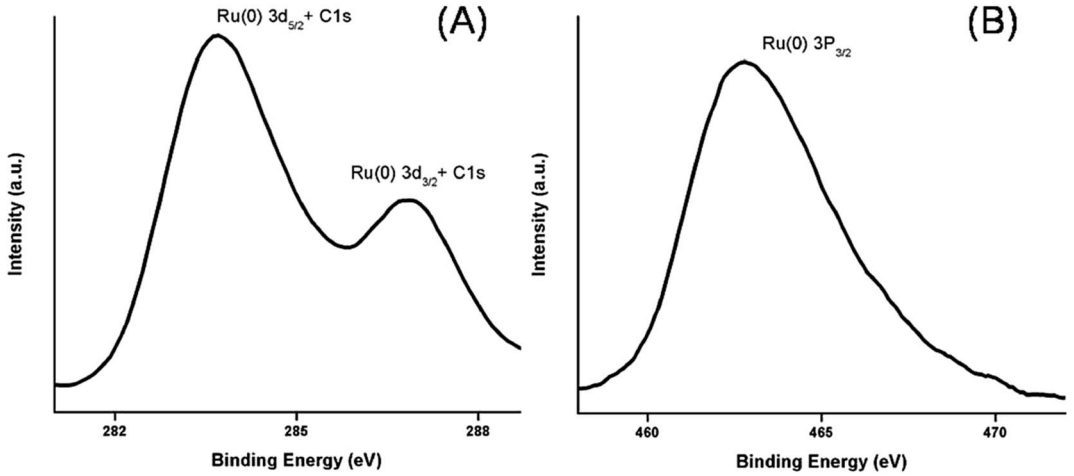

Fig. 5 XPS analysis of carbon nanodot supported Ru nanodots (A) 3d region and (B) 3p region.

peak found at around $2\theta = 25^\circ$ and this is an indicative of a disordered (amorphous) carbon (Fig. S4, ESI†).

Synthesis of Ru nanodots by using carbon nanodots as a template

The presence of carboxyl and/or hydroxyl functionalities in carbon nanodots can act as a support for Ru nanodot synthesis. As schematically illustrated in Scheme 2, at first, the reaction was conducted by dispersing Ru^{+3} salt in the aqueous solution of pre-synthesized carbon nanodots and these were then reduced to form Ru nanodots by using sodium borohydride (as a reducing agent).

Characterization of carbon nanodot supported Ru nanodots

It is evident from the TEM image (Fig. 3B) that these Ru nanodots (RuNDs) are almost spherical and most of them are also associated with the carbon nanodots. The particle distribution diagram (Fig. S5, ESI†) shows a narrow range of size distribution in 1–4 nm with a maximum population in the range of 2–3 nm. The presence of well resolved lattice planes throughout the particle implies the single crystalline nature of the RuNDs. The crystalline nature of the Ru nanodot is also in good agreement with the obtained XRD pattern of these carbon nanodot supported Ru nanodots (Fig. 4). The diffraction peaks are centered at $2\theta = 43.8$, 69.1 and 78.4, and these are consistent with those for face centered cubic (fcc) Ru(0) crystals. These diffraction peaks correspond to the (101), (110), and (103) Miller indices of Ru(0) nanoparticles, respectively. The diffraction peak at $2\theta = 43.8$ corresponds to the d-spacing 2.05 Å of fcc Ru(0) crystals. Besides XRD, XPS analysis was also carried out to confirm the Ru(0) state (Fig. 5). Due to the overlap of the Ru 3d peak with C1s, it is very difficult to conclude the presence of the Ru(0) state under the scan of this region. However, the peak at 462.8 eV can readily be assigned to the $3p_{3/2}$ peak of Ru(0) and therefore, it can be said that metallic [Ru(0)] particles are formed. The formation of RuNDs is also evident from the EDS analysis (Fig. S6, ESI†).

Organic azide reduction study by using carbon nanodot supported Ru nanodot catalyst

These well dispersed Ru nanodots supported on carbon nanodots are stable. The presence of functional groups in fluorescent carbon nanodots helps to entrap and stabilize Ru nanodots by using a Ru/CND hybrid nanodot system. This hybrid material has been examined as a potential catalyst for catalytic hydrogenation of various organic azide derivatives. To optimize the reaction conditions, a number of experiments have been carried out by using phenylazide as a standard. It is found that the reaction time and the % of yield are greatly affected by the amount of catalyst used (Table 1). Though 5 mol% of catalyst gives a good yield, the time of completion is quite high (24 h). The optimum results are obtained when 50 mol% catalysts are used. The reaction does not proceed at room temperature. At 60 °C the reaction gives a very low yield even after 24 h of the reaction. However, the best result is obtained, when the temperature is adjusted to 100 °C. The reaction is finished within 2.5 h under such conditions. We have also tested the reaction in several solvents; water gives the best result (Table 1). The role of hydrazine is also very crucial. To check this, the reaction is carried out in the absence of hydrazine under similar conditions; however, a desirable yield was not obtained under

Table 1 Standardization of organic azide reduction conditions[a]

Entry	Solvent	Temperature	Catalyst (mol %)	Time (hr)	Yield (%)
1	H_2O	rt	50	24	No reaction
2	H_2O	60 °C	50	24	18
3	H_2O	100 °C	50	2.5	95
4	H_2O	100 °C	10	2.5	70
5	H_2O	100 °C	5	2.5	59
6	H_2O	100 °C	5	24	63
7	DMF	100 °C	50	2.5	36
8	Toluene	100 °C	50	2.5	12

[a] Phenylazide was taken as a substrate to optimize the reaction conditions in the presence of hydrazine.

such conditions. Thus, in a typical procedure azide compounds are successfully reduced to their corresponding amines in the presence of hydrazine and a catalytic amount of Ru/CND (as a nanocatalyst) in water at 100 °C within 2–4 hours. Under such optimized conditions a series of organic azides are reduced to their corresponding amines (Table 2). The catalyst does not bring about any change to other functionalities including hydroxyl, ether, carboxylic acid, ester, alkyl, halide and sulfonyl group(s) present in their corresponding azides. This indicates the good chemoselectivity of the nanocatalyst towards the azide moiety. We have also examined the catalytic activity of individual nanodots (carbon nanodots and Ru nanodots separately). However, in none of these cases, better activity was found compared to that of the Ru/CND catalyst (Table S1†). Carbon nanodots (CNDs) alone do not show any catalytic reduction under similar conditions. The Ru nanodots (prepared by using glycylglycine peptide as a capping ligand, without using carbon nanodots as a stabilizer) exhibit less catalytic efficiency than the Ru nanodot catalyst prepared with carbon nanodots (*i.e.* the hybrid nanodots). The TEM image (Fig. S7, ESI†) of the peptide stabilized Ru nanodots (Ru/pep) show that the most of these particles are aggregated and possess larger sizes. This suggests that an inefficient stabilization of Ru nanodots occurs, if peptide is used alone as a stabilizing agent. Such agglomeration of Ru nanodots is attributed to the poorer catalytic efficiency of Ru/pep compared to that of the hybrid Ru/CND catalyst. The Ru/CND nanocatalyst has been recovered through filtration followed by thorough washing with water and methanol and then drying. This recovered dried catalyst can then be reused up to 6 times (Fig. S8, ESI†). However, the % of yield of the reaction decreases significantly after the 6th cycle. The loss of catalytic activity can be attributed to the loss of some amount of catalyst due to common separation techniques and/or agglomeration of the catalyst after each cycle. There are also a few examples of the ruthenium complex based catalyst for azide reduction. Liu and co-workers have reported the photocatalyzed reduction of azides using catalytic $[Ru(bpy)_3]_2^+$ and stoichiometric *i*-Pr_2NEt/HCOOH/Hantzsch ester or ascorbate or NADPH (nicotinamide adenine dinucleotide phosphate) as a reducing agent in dichloromethane or mixed solvent 1 : 1 CH_3CN/H_2O.[57] Their developed method is highly chemoselective towards azide functionality and it also exhibits good compatibility towards biologically important substrates. Leung and co-workers have synthesized a ruthenium ion based complex that can catalyze the 4-nitrophenyl azide to 4-nitroaniline reduction in the presence of cyclohexene.[58] However, none of these examples included the recyclability of the catalyst. On the other hand, this hybrid Ru/CND catalyst is insoluble in water owing to its highly hydrophobic nature and this enables the effective removal of the catalyst, so that it can be reused for subsequent reactions. Such a recycling procedure can be extended up to 6 times and it shows a significant yield even after the 6th cycle (78%). Although the Ru/CND catalyst shows comparable chemoselectivity and yield (%) with the aforementioned catalyst, the use of the Ru/CND catalyst is more advantageous in terms of recyclability of the catalyst when compared to the other previously mentioned catalysts.

Table 2 Reduction of organic azides by Ru/CND catalyst in presence of hydrazine monohydrate in water[a]

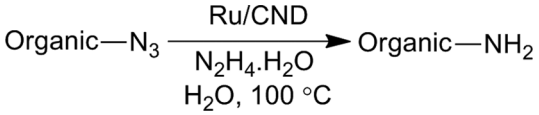

Entry	Substrate	Product	Time (h)	Yield[b] (%)
1	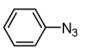		2.5	95
2	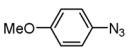	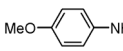	2.5	90
3	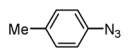	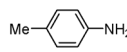	3	87
4	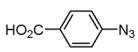	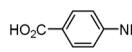	3.5	72
5	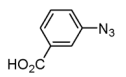	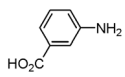	2.5	90
6	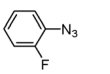		2.5	92
7	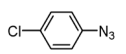	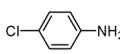	2.5	94
8	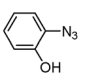		3.5	74
9	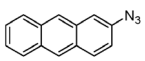	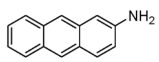	4	69
10	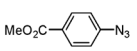	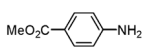	2.5	92
11	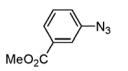	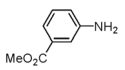	2.5	90
12	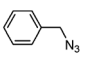		2	89
13	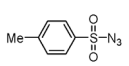	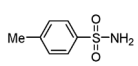	2	93
14	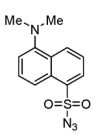	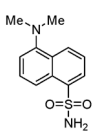	2.5	89

[a] Reaction conditions: organic azide (1 mmol), $N_2H_4 \cdot H_2O$ (5 mmol), Ru/CND catalyst (50 mol%) water (5 mL), 100 °C. [b] Isolated yield (determined by ^1H and ^{13}C NMR).

Conclusions

In this study, an elegant strategy has been used to synthesize peptide functionalized carbon nanodots and these as-prepared carbon nanodots act as a template to obtain Ru nanodots containing hybrid nanodots in the presence of Ru^{+3} ions and sodium borohydride. Interestingly, these hybrid nanodots have been used as a potential nanocatalyst for the chemoselective reduction of organic azides to their corresponding amines in the presence of other functional groups in aqueous medium at

ambient temperature (100 °C) with good yields and high recyclability. The formation of hybrid nanodot containing metal nanoparticles with interesting catalytic properties holds a future promise for creating novel functional materials for catalysis and other interesting applications.

Acknowledgements

A. Biswas thanks the CSIR, New Delhi, India, for financial assistance. We also gratefully acknowledge the DST Unit of Nanoscience at IACS for providing access to their XPS facility. We are thankful to Mr. Supriyo Chakraborty of MLS Unit of IACS for his expertise and patience to record good TEM images.

References

1 M.-M. Titirici, R. J. White, N. Brun, V. L. Budarin, D. S. Su, F. del Monte, J. H. Clark and M. J. MacLachlan, *Chem. Soc. Rev.*, 2015, **44**, 250.
2 A. Rahy, C. Zhou, J. Zheng, S. Y. Park, M. J. Kim, I. Jang, S. J. Cho and D. J. Yang, *Carbon*, 2012, **50**, 1298.
3 X. Wen, P. Yu, Y.-R. Toh, X. Ma and J. Tang, *Chem. Commun.*, 2014, **50**, 4703.
4 J. Jeong, M. Cho, Y. T. Lim, N. W. Song and B. H. Chung, *Angew. Chem., Int. Ed.*, 2009, **48**, 5296.
5 A. Krueger, *Adv. Mater.*, 2008, **20**, 2445.
6 K. Welsher, Z. Liu, S. P. Sherlock, J. T. Robinson, Z. Chen, D. Daranciang and H. Dai, *Nat. Nanotechnol.*, 2009, **4**, 773.
7 J. Nanda, A. Biswas, B. Adhikari and A. Banerjee, *Angew. Chem., Int. Ed.*, 2013, **52**, 5041.
8 V. Gupta, N. Chaudhary, R. Srivastava, G. D. Sharma, R. Bhardwaj and S. Chand, *J. Am. Chem. Soc.*, 2011, **133**, 9960.
9 B. Adhikari, A. Biswas and A. Banerjee, *ACS Appl. Mater. Interfaces*, 2012, **4**, 5472.
10 J. Peng, W. Gao, B. K. Gupta, Z. Liu, R. Romero-Aburto, L. Ge, L. Song, L. B. Alemany, X. Zhan, G. Gao, S. A. Vithayathil, B. A. Kaipparettu, A. A. Marti, T. Hayashi, J.-J. Zhu and P. M. Ajayan, *Nano Lett.*, 2012, **12**, 844.
11 M. Sevilla, L. Yu, L. Zhao, C. O. Ania and M.-M. Titirici, *ACS Sustainable Chem. Eng.*, 2014, **2**, 1049.
12 S. Zhuo, M. Shao and S.-T. Lee, *ACS Nano*, 2012, **6**, 1059.
13 A. Biswas and A. Banerjee, *Chem.–Asian J.*, 2014, **9**, 3451.
14 A. Suryawanshi, M. Biswal, D. Mhamane, R. Gokhale, S. Patil, D. Guin and S. Ogale, *Nanoscale*, 2014, **6**, 11664.
15 D. Pan, J. Zhang, Z. Li, C. Wu, X. Yan and M. Wu, *Chem. Commun.*, 2010, **46**, 3681.
16 H. Li, Z. Kang, Y. Liu and S.-T. Lee, *J. Mater. Chem.*, 2012, **22**, 24230.
17 S. N. Baker and G. A. Baker, *Angew. Chem., Int. Ed.*, 2010, **49**, 6726.
18 P. G. Luo, F. Yang, S.-T. Yang, S. K. Sonkar, L. Yang, J. J. Broglie, Y. Liu and Y.-P. Sun, *RSC Adv.*, 2014, **4**, 10791.
19 Y. Yang, J. Cui, M. Zheng, C. Hu, S. Tan, Y. Xiao, Q. Yang and Y. Liu, *Chem. Commun.*, 2012, **48**, 380.
20 Z.-C. Yang, M. Wang, A. M. Yong, S. Y. Wong, X.-H. Zhang, H. Tan, A. Y. Chang, X. Li and J. Wang, *Chem. Commun.*, 2011, **47**, 11615.
21 K. Lawrence, F. Xia, R. L. Arrowsmith, H. Ge, G. W. Nelson, J. S. Foord, M. Felipe-Sotelo, N. D. M. Evans, J. M. Mitchels, S. E. Flower, S. W. Botchway, D. Wolverson, G. N. Aliev, T. D. James, S. I. Pascu and F. Marken, *Langmuir*, 2014, **30**, 11746.
22 A. B. Bourlinos, R. Zbořil, J. Petr, A. Bakandritsos, M. Krysmann and E. P. Giannelis, *Chem. Mater.*, 2012, **24**, 6.
23 D. Mazzier, M. Favaro, S. Agnoli, S. Silvestrini, G. Granozzi, M. Maggini and A. Moretto, *Chem. Commun.*, 2014, **50**, 6592.
24 X. Zhai, P. Zhang, C. Liu, T. Bai, W. Li, L. Dai and W. Liu, *Chem. Commun.*, 2012, **48**, 7955.
25 H. Wu, C. Mi, H. Huang, B. Han, J. Li and S. Xu, *J. Lumin.*, 2012, **132**, 1603.
26 S. K. Bhunia, A. Saha, A. R. Maity, S. C. Ray and N. R. Jana, *Sci. Rep.*, 2013, **3**, 1473.
27 S. Zhu, Q. Meng, L. Wang, J. Zhang, Y. Song, H. Jin, K. Zhang, H. Sun, H. Wang and B. Yang, *Angew. Chem., Int. Ed.*, 2013, **52**, 3953.
28 C. Zhu, J. Zhai and S. Dong, *Chem. Commun.*, 2012, **48**, 9367.
29 K. A. S. Fernando, S. Sahu, Y. Liu, W. K. Lewis, E. A. Guliants, A. Jafariyan, P. Wang, C. E. Bunker and Y.-P. Sun, *ACS Appl. Mater. Interfaces*, 2015, **7**, 8363.
30 A. Zhu, Q. Qu, X. Shao, B. Kong and Y. Tian, *Angew. Chem., Int. Ed.*, 2012, **51**, 7185.
31 M. Vedamalai, A. P. Periasamy, C.-W. Wang, Y.-T. Tseng, L.-C. Ho, C.-C. Shih and H.-T. Chang, *Nanoscale*, 2014, **6**, 13119.
32 Y. Dong, R. Wang, G. Li, C. Chen, Y. Chi and G. Chen, *Anal. Chem.*, 2012, **84**, 6220.
33 L. Zhou, Y. Lin, Z. Huang, J. Ren and X. Qu, *Chem. Commun.*, 2012, **48**, 1147.
34 H. Li, X. He, Z. Kang, H. Huang, Y. Liu, J. Liu, S. Lian, C. H. A. Tsang, X. Yang and S.-T. Lee, *Angew. Chem., Int. Ed.*, 2010, **49**, 4430.
35 S. Sahu, B. Behera, T. K. Maiti and S. Mohapatra, *Chem. Commun.*, 2012, **48**, 8835.
36 S. Qu, X. Wang, Q. Lu, X. Liu and L. Wang, *Angew. Chem., Int. Ed.*, 2012, **51**, 12215.
37 J. Wang, C.-F. Wang and S. Chen, *Angew. Chem., Int. Ed.*, 2012, **51**, 9297.
38 H. K. Sadhanala, J. Khatei and K. K. Nanda, *RSC Adv.*, 2014, **4**, 11481.
39 M. Liu and W. Chen, *Nanoscale*, 2013, **5**, 12558.
40 M. Cametti and Z. Džolić, *Chem. Commun.*, 2014, **50**, 8273.
41 A. Biswas and A. Banerjee, *Soft Matter*, 2015, **11**, 4226.
42 W. J. Peveler, J. C. Bear, P. Southern and I. P. Parkin, *Chem. Commun.*, 2014, **50**, 14418.
43 S. Roy, A. Baral and A. Banerjee, *Chem.–Eur. J.*, 2013, **19**, 14950.
44 V. Polshettiwar and R. S. Varma, *Green Chem.*, 2010, **12**, 743.
45 S. Alayoglu, A. U. Nilekar, M. Mavrikakis and B. Elchhorn, *Nat. Mater.*, 2008, **7**, 333.
46 P. P. Sarmah and D. K. Dutta, *Green Chem.*, 2012, **14**, 1086.
47 D. V. Jawale, E. Gravel, C. Boudet, N. Shah, V. Geertsen, H. Li, I. N. N. Namboothiri and E. Doris, *Chem. Commun.*, 2015, **51**, 1739.

48 M. Zahmakıran, M. Tristany, K. Philippot, K. Fajerwerg, S. Özkar and B. Chaudret, *Chem. Commun.*, 2010, **46**, 2938.
49 D. Gonzalez-Galvez, P. Lara, O. Rivada-Wheelaghan, S. Conejero, B. Chaudret, K. Philippot and P. W. N. M. van Leeuwen, *Catal. Sci. Technol.*, 2013, **3**, 99.
50 G. Chen, S. Desinan, R. Rosei, F. Rosei and D. Ma, *Chem. Commun.*, 2012, **48**, 8009.
51 S. A. Lawrence, *Amines: Synthesis, Properties and Applications*, Cambridge, 2006.
52 C. Gunanathan and D. Milstein, *Angew. Chem., Int. Ed.*, 2008, **47**, 8661.
53 K. Weissermel and H. J. Arpe, *Industrial Organic Chemistry*, Wiley-VCH, Weinheim, 1997, p. 295.
54 S. Ahammed, A. Saha and B. C. Ranu, *J. Org. Chem.*, 2011, **76**, 7235.
55 S. Pagoti, S. Surana, A. Chauhan, B. Parasar and J. Dash, *Catal. Sci. Technol.*, 2013, **3**, 584.
56 M. Warrier, M. K. F. Lo, H. Monbouquette and M. A. Garcia-Garibay, *Photochem. Photobiol. Sci.*, 2004, **3**, 859.
57 Y. Chen, A. S. Kamlet, J. B. Steinman and D. R. Liu, *Nat. Chem.*, 2011, **3**, 146.
58 H.-F. Ip, Y.-M. So, H. H. Y. Sung, I. D. Williams and W.-H. Leung, *Organometallics*, 2012, **31**, 7020.